# The World's Largest Metal Buried Bridge, Developed and Tested in Halifax Nova Scotia

Meckkey El-Sharnouby, PhD., P,Eng,
Senior Geostructural Engineer
Atlantic Industries Limited

Leszek Janusz, Ph.D., P.Eng,
CEO
ViaCon Group

John Newhook, Ph.D., P.Eng.
Professor, Faculty of Engineering
Dalhousie University

Paper prepared for the presentation
at the Structures Session

2019 TAC-ITS Canada Joint Conference, Halifax, NS

# PERFORMANCE OF THE LARGEST STEEL BURIED BRIDGE UNDER EARTH LOADS-A FULL-SCALE TEST


## ABSTRACT

Steel buried bridges have been an integral part of the Canadian infrastructure for decades. In 2019, the largest steel buried bridge in the world, the Shammal Bridge Crossing, was built for a transportation application in Dubai, UAE utilizing the Ultra-Cor Corrugation. The structure had a span of 32.39 m and a rise of 9.039 m which led to a spot on the Guinness World of Records. The structure was instrumented with strain gauges and deflection prisms. The full-scale test results demonstrated that the performance of the structure is satisfactorily and meets exceeds the targeted demand to capacity ratio.



Keywords: buried bridge, soil-structure interaction, CHBDC, Full-scale; deeper corrugation

## 1 INTRODUCTION

With the continuous increase in infrastructure needs and the existing constrained public budgets there is an increased emphasis on innovative solutions to build Canadian infrastructure. Steel buried bridges have been an integral part of the Canadian infrastructure for many decades. Steel buried bridges, also known as buried structures, comprise of a corrugated metal structure surrounded by engineered backfill. Buried bridges are used for various applications including, transportation, mining, tunneling and forestry.

Over the last three decades, buried bridges have been increasingly used for large span applications, providing at times a more cost-effective alternative to conventional bridges (TRB Committees AFF70 and AFS 40 2013). Their maximum spans have increased from 8 m to more than 25 m. The increased demand on these large span structures demonstrates the need to better understand their performance under various loading conditions, and to further evaluate and refine appropriate design methodologies used in their design.

Depending on the corrugation profile, corrugated metal structures are classified as shallow, deep corrugated, or deeper corrugated. CAN/CSA S6-14 (2014) assigns additional design considerations to deep- corrugated profiles due to its higher flexural rigidity. The deepest corrugation profile was developed in 2011. The profile has a pitch of 500 mm and rise of 237 mm (Williams et al. 2011). It is classified under CAN/CSA-G401-14 (2014) as Type III deep corrugated structure plate and as 'deeper corrugation' under CAN/CSA-S6-14. The first structure built with this profile was in 2011 for a highway underpass in Eastern Canada with a 13.3 m span and a 5.3 m rise (Vallee et al. 2014 and Vallee 2015).

Current equations in CAN/CSA-S6-14 (2014) are based mostly on finite element analysis by Duncan (1978). There is a need to re-examine the suitability of these equations for deep and very deep corrugated profiles and long span structures (Newhook 2017). Choi et al. (2004) compared the code equations to predictions by finite element analysis for spans up to 20 m Type II deep corrugated plate. They found that code equations are valid and a little conservative. Vallee (2015) instrumented the Type III corrugation structure with strain gauges and deflection prisms. Vallee (2015) found that the code simplified method can be very conservative for long span single radius arches and conservative for short span arches with relatively stiff plates.

In 2019, the largest steel buried structure in the world was built for a transportation application in United Arab Emirates. Utilizing the Type III corrugation, the structure has a span of 32.42 m and a rise of 9.57 m.

The Shammal Bridge near Dubai, United Arab Emirates (UAE), recently earned a Guinness World Record for having the world's largest metal buried bridge with a span of 32.42 m. The crossing consisted of three arches, as shown in Figure 1, two with the record span of 32.39m and one with 23.763 m.

The structures were instrumented with strain gauges and deflection prisms, and readings were taken during backfilling. In this paper, strain measurements and deformations of the structure during backfilling for one of the largest structures are presented. Stress and deformation results are presented and evaluated with the 2014 CHBDC's deformation and plastic hinge limit states.
deformations

## 2 STRUCTURE DETAILS

### 2.1 Structure Geometry

As stated above, the Shammal bridge crossing consists of three structures having a length of 12.076 m. The two identical structures are custom dual radius arches with inside span of 32.407 m and rise of 9.57 m, as shown in Figure 2. The structure geometry was custom designed to fit the project clearance requirements.

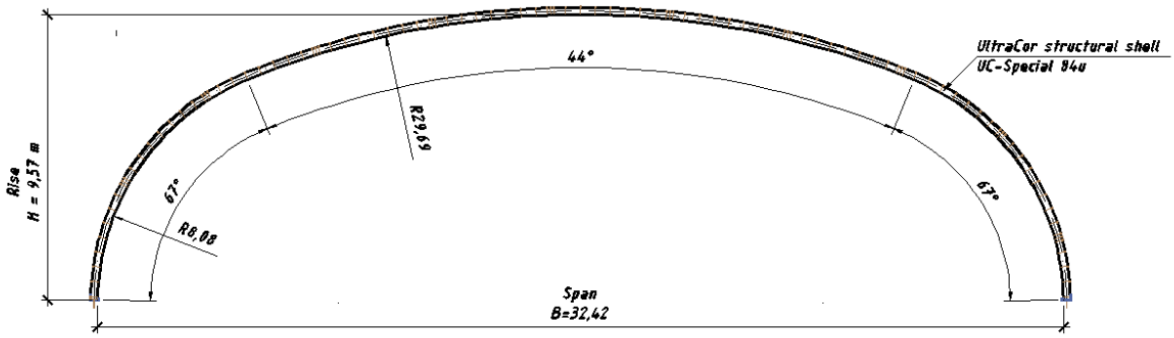


Figure 2: Structure geometry

### 2.2 Structural Plate Corrugated Steel

The corrugation profile of this structure is known as ‘Ultra-Cor’ which is designated under CAN/CSA G401-14 (2014) as ‘Type III corrugation’ and under CAN/CSA S6-14 (2014) as ‘deeper corrugation.’ The corrugation profile is 500 mm x 237 mm, as can be seen in Figure 3. The straight portion is called tangent while the curved portions are called valley and crest. Thickness of steel was 12 mm for the two large arches and 10 mm for the third arch. The mechanical properties are shown in Table 1. The

'deeper corrugation' offers more than three times the flexural rigidity compared to deep corrugation plates (381 mm x 140 mm) of the same thickness. The structure conforms to EN 10025-2 and EN 10149-2.

Table 1. Cross-section properties for the 500 x 237 mm profile

| Specified thickness, mm | Area, $mm^2/mm$ | Moment of inertia $mm^4/mm$ |
|---|---|---|
| 12 | 17.366 | 111217 |

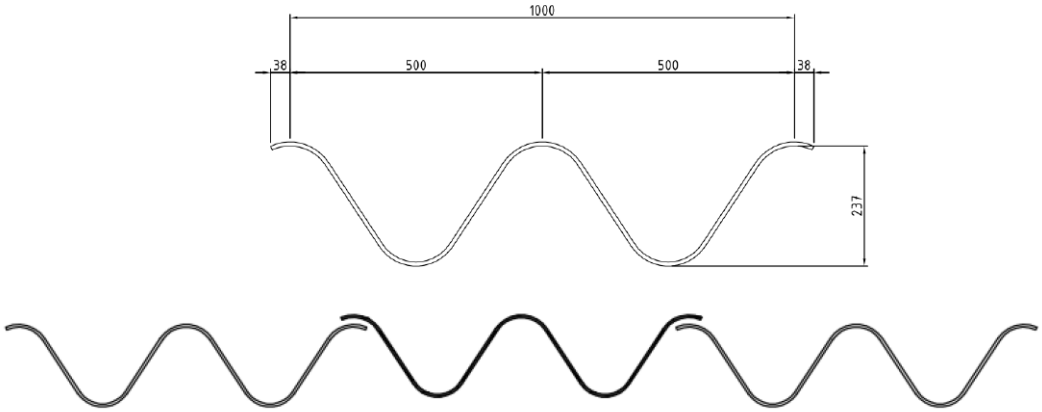


Figure 3. Corrugation profile of Type III corrugation, CAN/CSA S6-14

## 2.3 Corrosion Protection

The structure was protected with zinc coating conforming to EN ISO 1461. Additionally, the both sides of the structure were protected with epoxide layer and polyurethane layer which is applied after assembly of the structure.

# 3 FIELD TESTING

## 3.1 Instrumentation

All three structures were instrumented with strain gauges placed at 17 measurement points along the periphery of the structure, as shown in Figure 4. Gauges were placed on the inside surface of the structure, at the crest and the valley of the corrugation as shown in Figure 5.

Three-dimensional deformations of the steel structure were measured using a geodetic laser device. Fifty-one measuring points were arranged at seventeen individual points in three sections of the each arch. Location of the measurement points at the valley of the corrugation is shown in Figure 6. For each of the measuring points deformations were registered as changes between a fixed three reference points on the ground and the optical prisms installed on the steel plates.

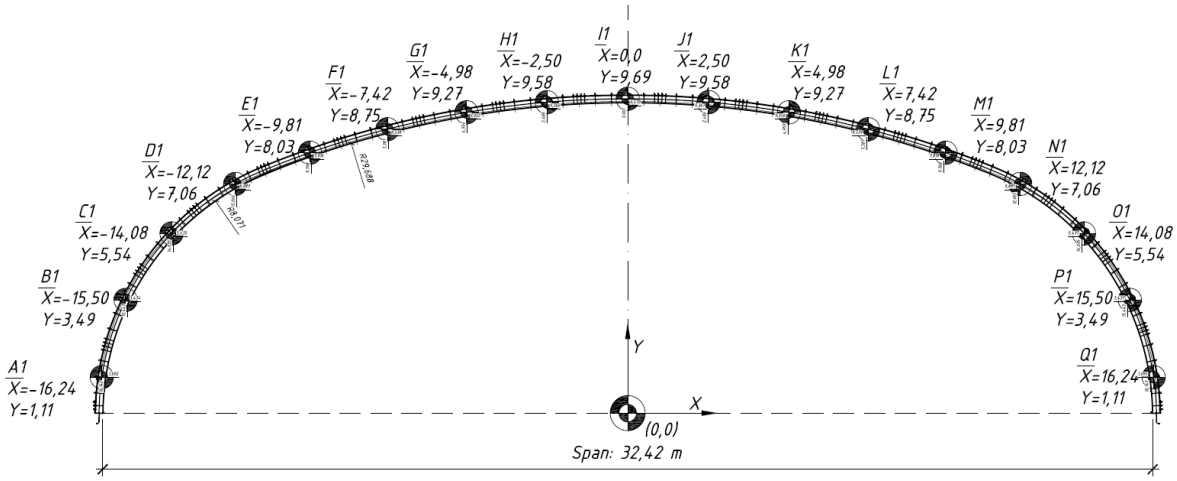


Figure 4. Location of strain gauges and deflection prisms along the structure periphery.

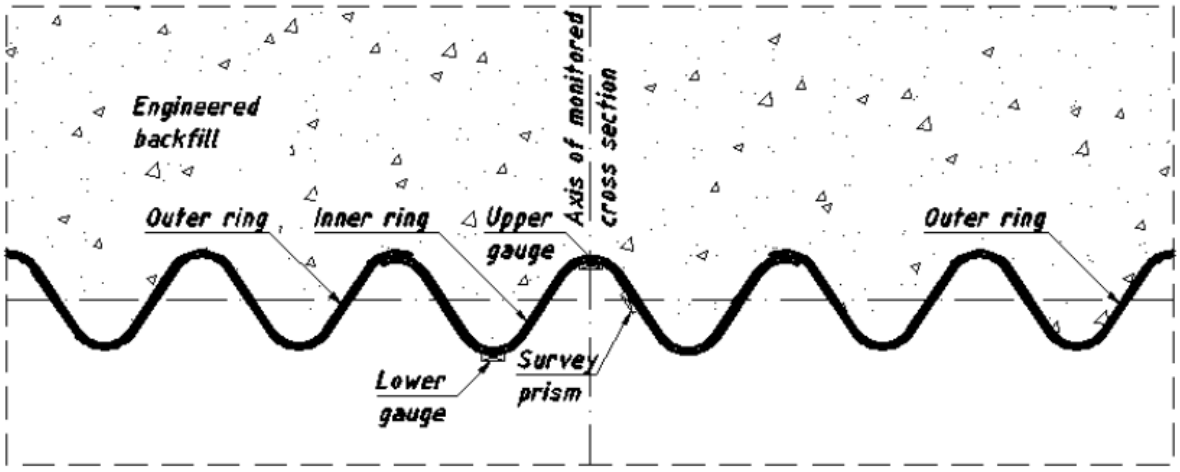


Figure 5: Position of gauges at each measurement location

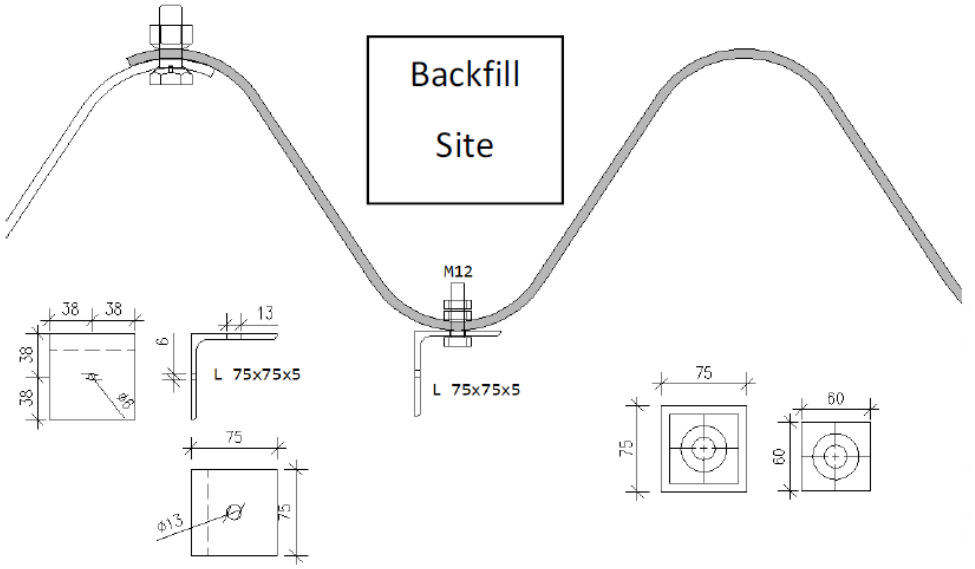

Figure 6. Deflection prisms locations at valley of corrugation.

### 3.2 Structural Assembly

The structure had 12 rings with each ring consisting of several plates. The structure was assembled as per industry standards. First, odd numbered rings were pre-assembled then lifted and secured into place; first ring can be seen in Figure 7. Remaining plates were installed plate by plate by bolting the plates to the fully erected adjacent rings as can be seen in Figure 8 and 9. Assembly of three arches took 24 working days.


Figure 7 Photo for first ring assembly.


Figure 8: Photo of erection of first three rings

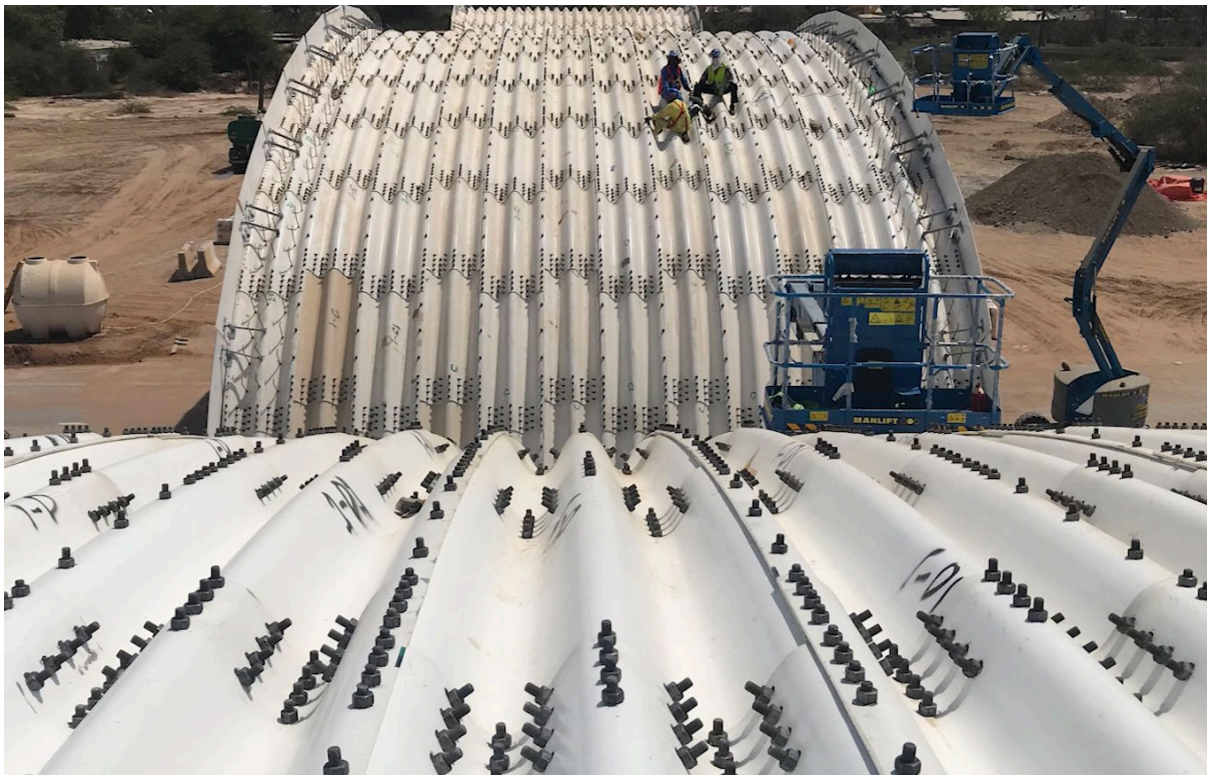

Figure 9. Photo for structure assembly near completion

### 3.3 Backfill

The backfill material for the structure complied with the following requirements, GW/SW material Unified Soil Classification System (ASTM 2487-11 2015), uniformity coefficient, Cu ≥ 6.0, coefficient of gradation, 1.0 ≥ Cc ≥ 3.0, unit weight, 20.5 kN/m3 ≤ γ ≤ 22 kN/m3. The backfill material is to be placed and compacted with a maximum lift thickness of 300 mm, compacted to more then 98% standard proctor density ASTM D1557 (2015).

Due to access constraints, controlled low strength concrete was used to fill in between the two identical structures up to 3.25 m. To control peaking, a special feature wire mesh reinforcement was installed along the rise of the structures, as shown in Figure 10.

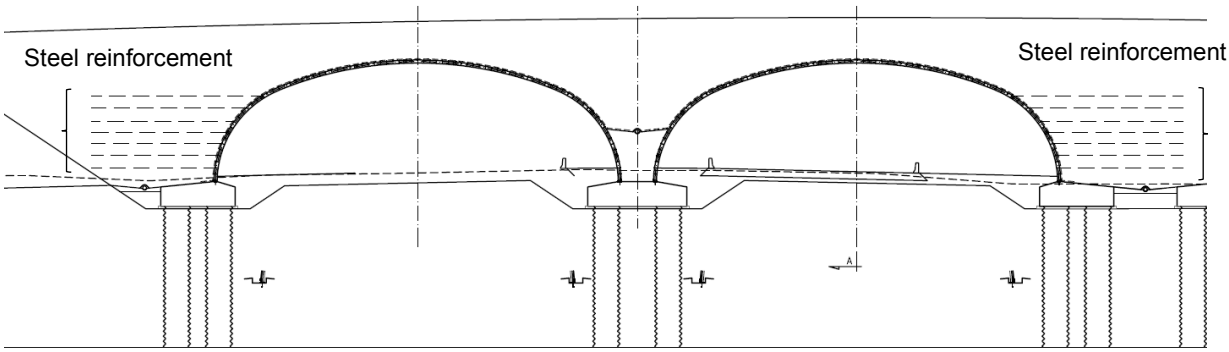


Figure 10. Steel mesh along the rise of the structure.

## 4 RESULTS

### 4.1 Structure Deformations

Deformation monitoring during construction is a regular practice in buried soil-metal structures. Deformations serve as an indication of construction quality and structure stress. CAN/CSA S6-14 (2014) clause 7.6.5.2 states upward deflection shall not exceed 2% of the rise unless Approved. According to the relevant code commentary (CAN/CSA S6.1-14 2014), this limit is based on empirical consideration rather than analysis. CAN/CSA S6-14 (2014) does not impose limits on lateral movements of these structures. El-Sharnouby et. al (2016) observed satisfactorily performance associated higher deflections in previous large span Ultra-Cor structures. El-Sharnouby et. al recommends a larger deflection limit in the CHBDC limit. Recognizing this work, the 2019 CHBDC permits crown deflections in excess of 2% when the engineer has determined it is not detrimental to the structure . It is worth noting that there are no theoretical or empirical methods in the CAN/CSA S6-14 to estimate structure deflection. Deformations are commonly predicted through using finite element analysis or past performance.

Figure 11 shows the deformation of the crown during construction. Vertically upward movements are expressed in positive units and vertically downward movements are expressed in negative units. The structure experienced negligible deformation up to 6 m of backfill height. As backfill height increases, the crown moved upwards with a maximum deformation of 105 mm when the backfill height reached the structure top elevation. As backfilling continued with fill placed above the crown, the structure displayed downward movement. At full backfill height, maximum downward movement was measured at -78 mm at the crown.

Figure 12 shows horizontal deformations are towards the inside of the structure. As backfill is placed and compacted against the structure it applies pressure to the structure's sidewalls which results in the inward deformation. As fill is placed above the structure the top of the structure deforms downwards and the sidewalls move into the soil. Appreciable horizontal deformations are not observed until a backfill height of 3 m. Sidewall (haunch) deformation increased steadily until backfill reached the crown elevation. Inward deflection measured at 27 mm when backfill was at the crown. The sidewall remained inward at end of construction at a deflection of 12 mm. The observed trend of inward movement at the haunch and upward movement at the crown is typical during backfilling of soil-metal buried structures.
Maximum upward movement during construction is 1.08 % of the rise which is less than the 2% CHBDC code limit. El-Sharnouby et al. (2016) reported the upward deflection of a 26.5 m span and 9.0 m rise structure was 2.5% of the structure rise compared to 1.08% for the 32.4 m span and 9.0 m rise Dubai structure. The smaller crown deformation on the Dubai structure is directly associated with the impact of the steel reinforcement special feature which reduced the peaking deformation and structure stress.

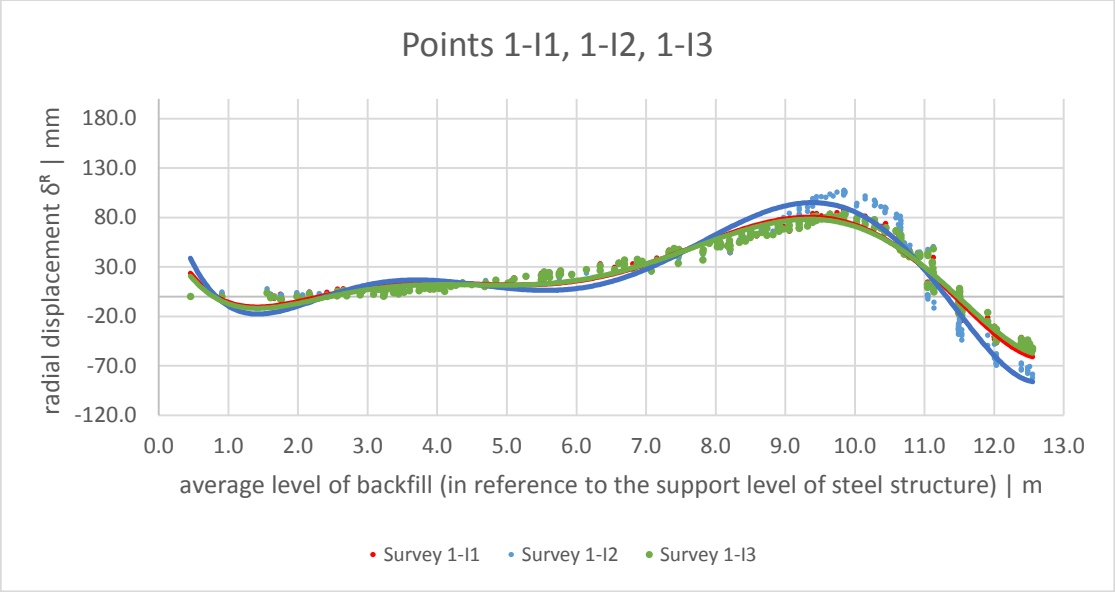


Figure 11. Measured deflection at crown location during test

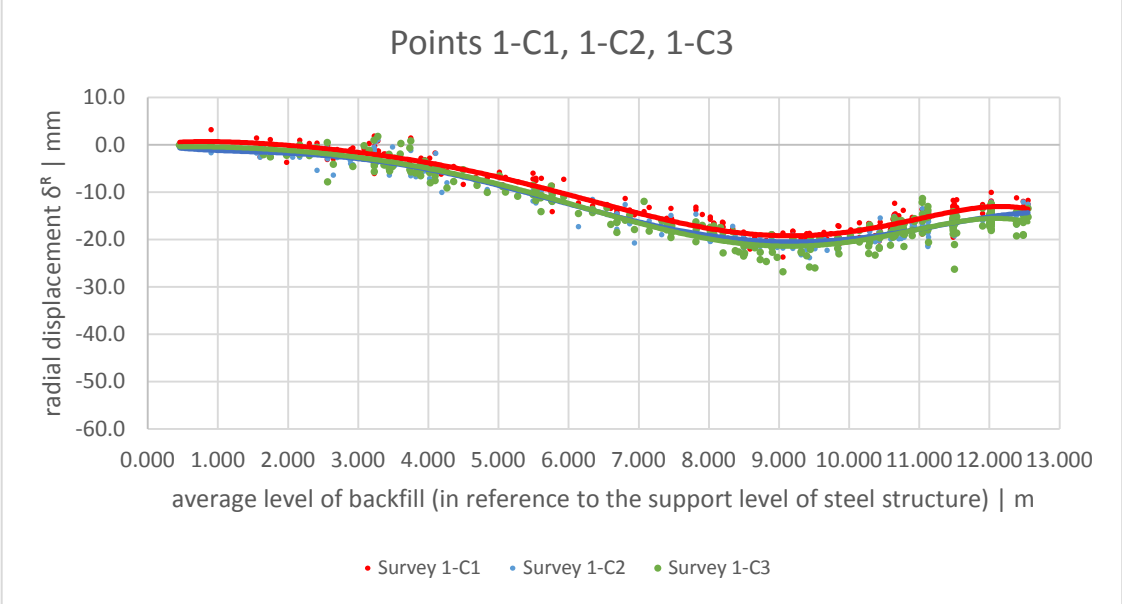


Figure 12.Measured deflection at haunch location during test.

### 4.2 Stress Distribution

Strain gauges data collected was throughout the construction process wasconverted into stress. Figure 13 shows the stress distribution along the structure periphery for a backfill height at the crown elevation. Red represents the stress in the inside crest of the corrugation and green represents the stress in the inside valley of the corrugation. Structure stress when backfill is at the crown elevationranged from 10 MPa to a maximum of 156 MPa, which is

well below the structure's capacity. This translates to a CHBDC's demand capacity ratio for plastic hinge of 31.5, which is less substantially lower than the limit of 1.00.

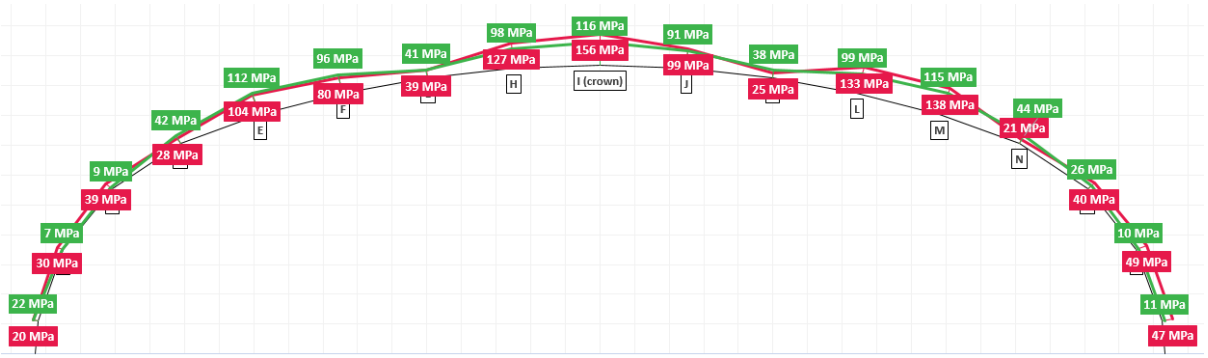


Figure 13. Stress distribution at backfill height at crown elevation.

Figure 14 shows the stress distribution at full backfill height of 12.63 m (or approximately 3 m above the crown). The stress level ranges from 52 MPa to 157 MPa. The maximum stress level is observed at the crown area and ranged from 50 MPa to 245 MPa. This translates to a CHBDC's demand capacity ratio for plastic hinge of 49%, which is less substantially lower than the limit of 1.00.

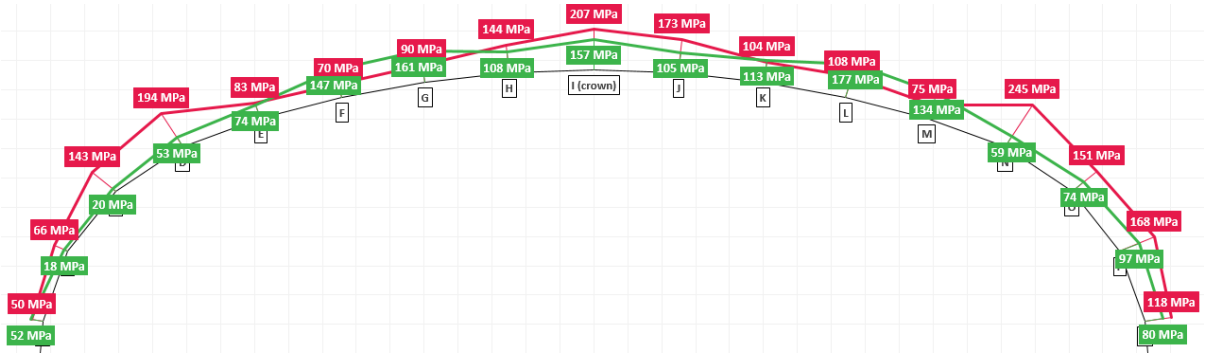


Figure 13. Stress distribution at backfill height at crown elevation.

## 5 CONCLUSIONS

The Shammal grade separation bridge is part of the UAE's mega RAK Ring Road project that is establishing a more robust transportation corridor between the northern Emirate of Ras Al Khaimah (RAK) and the rest of the Emirates. This crossing recently earned a Guinness World Record for having the world's largest metal buried bridge with a span of 32.39 m.

For such an innovative and significant span, the structure was health monitored during construction with the assistance of deformation and strain gauges. Strain gauge data was analyzed and converted

to stress. The CHBDC's plastic hinge limit state demand to capacity ratio was less than 49%, suggesting there showing high levels of safety margins in the structure. The maximum vertical deflection was 1.08% of the rise, less than the CAN/CSA S6-14 limit of 2% during construction. This ratio demonstrated the effectiveness of the steel reinforcement special feature. The performance criterion during construction was satisfied with substantial safety margin.

This paper demonstrated that metal buried structures are a viable option for long span bridges and is worth consideration in Canadian infrastructure.

**References**


ASTM A796/A796M-15A. 2015. Standard Practice of Structural Design of Corrugated Steel Pipe, Pipe-Arches and Arches for Storm and Sanitary Sewers and other Buried Application. *American society of testing and materials*. West Conshohocken, PA, USA.

ASTM D1557-12e1 2015. D1557-12e1 Standard Test Methods for Laboratory Compaction Characteristics of Soil Using Modified Effort. *American society of testing and materials*. West Conshohocken, PA, USA.

ASTM D2487-11. 2015. Standard Practice for Classification of Soil for Engineering Purposes (Unified Soil Classification System). *American society of testing and materials*. West Conshohocken, PA, USA.

CAN/CSA S6-14. 2014. Canadian Highway Bridge Design Code Canadian Standard Association. *Canadian Standard Association*. Mississauga, ON, Canada.

CAN/CSA-S6.1-14. 2014. Canadian Highway Bridge Design Code commentary Canadian Standard Association. *Canadian Standard Association*. Mississauga, ON, Canada.

CAN/CSA G401-14. 2014. Corrugated steel pipe products Canadian Standard Association. *Canadian Standard Association*. Mississauga, ON, Canada.

Choi, D.-H, Kim, G.-N and Byrne, P. 2004. Evaluation of the Moment Equation in the 2000 Canadian Highway Bridge Design Code for Soil-Metal Arch Structures. *Canadian journal of civil engineering*. 31: 281-291.

El Sharnouby, M.M, Newhook, J. and El Naggar, H. 2016. Performance of the largest flexible buried structure during construction- Full-scale test. Proceedings of the 69th Canadian Geotechnical Conference, Vancouver, Oct. 2-5, Paper 3765.

Duncan, J. 1978. Soil Culvert Interaction Method for Design of Metal Culverts. Transportation research record 678. *Transportation research board*, *National research council.* Washington, DC, USA.

Newhook.J. 2017. CHBDC buried structures: challenges in keeping pace with practice and innovation. Proceedings of the 3rd European Conference on Buried Flexible Steel Structures, Rydzyna, April 24-25, Archives of Institute of Civil Engineering, Poland.

TRB AFF70 and AFS40. 2013. Advantages to Culvert Selection for River and Road Crossings. Transportation Research Board 92nd Annual Meeting. Washington, D.C.: Transportation Research Board.

Vallee, J.H.F 2015. Investigation of Increased Wall Stiffness on Load Effect Equations for Soil Metal Structures. *Master of applied science these*. Dalhousie University, NS, Canada.

Vallee, J., Newhook, J.P. and Ford, W. 2014. Construction and Monitoring of Soil-Steel Bridge with Deeper Corrugated Plates. Proceedings of 9th International Conference on Short and Medium Span Bridges Calgary, Alberta, Canada, July 15-18, 2014. Paper 466.

Williams, K., MacKinnon, S. and Newhook, J. 2012. New and Innovative Developments for Design and Installation of Deep Corrugated Flexible Steels Structures. *The 2nd European conference on buried flexible structures.* Poznan, Poland.

Machelski, Cz., Janusz, L,, Tomala, P,, Williams, K., Deformation parameters of UltraCor steel plate in a soil-steel structure, TRB 2018 Washington DC.

Cz. Machelski P. Tomala B.Kunecki LKorusiewicz K.Williams M. El Sharnouby - UltraCor 1-st realization in . *The 3rd European conference on buried flexible structures.* Poznan, Poland 2017.